Pyrazole-inducible proteins in DBA/2 mouse liver bind with high affinity to the 3′-untranslated regions of the mRNAs of coumarin hydroxylase (*CYP2A5*) and c-*jun*

Monika THULKE-GROSS*, Manfred HERGENHAHN*[1], Anne TILLOY-ELLUL†, Matti LANG‡ and Helmut BARTSCH*

*Division of Toxicology and Cancer Risk Factors, Deutsches Krebsforschungszentrum (DKFZ), D-69120 Heidelberg, Germany, †Unit of Molecular Toxicology, International Agency for Research on Cancer, F-69372 Lyon, France, and ‡Division of Biochemistry, Faculty of Pharmacy, University of Uppsala, Box 578, Uppsala, Sweden

An important mechanism in the up-regulation of cytochrome *P*-450 2A5 (CYP2A5, coumarin hydroxylase, Coh) is the stabilization of the corresponding mRNA; some evidence suggests that proteins binding to CYP2A5 mRNA may be involved in this stabilization. Here we report that pyrazole, a well known inducer of *CYP2A5* and stabilizer of its message, enhances the binding of a set of proteins to ^{32}P-labelled 3′-untranslated region (3′UTR) of *CYP2A5* to give ^{32}P-labelled bands of apparent molecular mass 37/39, 45/48 and 70/72 kDa after UV cross-linking/RNase cleavage; in addition, we found different proteins binding to other parts of CYP2A5 mRNA. The 70/72 kDa bands are also formed with the 3′UTR of c-*jun*. The inducible proteins are found in different cellular subfractions at different concentrations, with a maximum of five-fold induction of binding activity in microsomes. When a gel-mobility-shift assay was combined with UV cross-linking to resolve different pyrazole-inducible RNA–protein complexes into single RNA-binding protein bands, the smallest complex contained a double band of 37/39 kDa, 45/48 kDa bands, 70/72 kDa bands, and additional weaker bands at higher molecular masses (around 120 kDa). This composition was found also for all other complexes detected by gel-mobility-shift assay; occasionally, bands at higher molecular masses were also observed. The proteins of the smallest complex might therefore represent a core with which other proteins interact to build up larger complexes. Binding of proteins 37/39 kDa and 70/72 kDa was located to a 20-base loop and adjacent sequences in a 70 nt AU-rich region of the 3′UTR of the *CYP2A5*. Based on our previous evidence, this 70-nt sequence may play an important role in the stabilization and processing of the message.

INTRODUCTION

CYP2A5 (cytochrome *P*-450 2A5; coumarin hydroxylase, Coh) in mice (CYP2A6 in humans) metabolizes several carcinogens including *N*-dialkylnitrosamines and aflatoxin B1 [1–9]. Interestingly, several stress conditions induce CYP2A5 in mouse liver, for example, fasting or a number of chemical inducers such as pyrazole, phenobarbital, hexachloro-1,3-butadiene, cobalt salts, cocaine and inorganic tin (see [9,10]). In addition, chronic inflammation has been shown to induce the enzyme in *Opisthorchis viverrini*-infested hamsters and HBseAg-transgenic mice [11,12]; in both systems, induction of the enzyme was associated with elevated aflatoxin–DNA adduct formation. Enhanced Coh levels in humans in North-East Thailand may be associated with aflatoxin-induced cholangiocarcinomas subsequent to infection by the liver fluke *Opisthorchis viverrini* [13], and liver from some kidney transplant donors and biopsies from patients with Hepatitis B virus (HBV)-associated hepatitis and cirrhosis showed enhanced levels of Coh [8,14].

Both, transcriptional and post-transcriptional events are involved in the regulation of CYP2A5; for example, phenobarbital is a transcriptional activator of the *CYP2A5* gene whereas pyrazole and some other toxic compounds may increase its expression by increasing the half-life of the mRNA [15–17]. At present, the mechanism of CYP2A5 mRNA stabilization is not well understood. Recently, however, a 44 kDa pyrazole-inducible protein has been described by UV cross-linking to the 3′-untranslated region (3′UTR) of *CYP2A5* and there is some evidence that this protein may be involved in stabilization and processing of the message [18].

The aim of the present work was to expand the studies on proteins which interact with CYP2A5 mRNA. By using gel-mobility-shift assays (GMSA) in combination with UV-cross-linking, we have shown that several pyrazole-inducible proteins bind with high affinity to CYP2A5 mRNA; in addition, two of them bind strongly to the 3′UTR of c-*jun*, a protein that is also induced by various forms of stress [19,20].

MATERIALS AND METHODS

Animals

Male DBA/2N mice provided by Charles River, Sulzfeld, Germany (~ 6 weeks old) were injected intraperitoneally with either PBS alone or with pyrazole dissolved in PBS at a dose of 150 mg/kg (200 μl maximum injection volume) for 3 consecutive days. The animals were killed 24 h after the last injection and the liver was removed.

Preparation of subcellular fractions

Excised mouse liver was homogenized in a Dounce homogenizer in ice-cold homogenization buffer (10 mM Hepes, pH 7.8/1.5 mM $MgCl_2$/15 mM KCl/2 mM dithioerythritol (DTE)/0.25 M sucrose containing the following proteinase inhibitors (Boehringer, Mannheim, Germany): 250 μg/ml of Pefabloc, 5 μg/ml of leupeptin, 5 μg/ml of pepstatin, 1 μg/ml of aprotinin).

Abbreviations used: CDS, coding sequence; Coh, coumarin hydroxylase; CYP2A5, cytochrome *P*-450 2A5; DTE, dithioerythritol; Ex 1-3, exon 1-3; GMSA, gel mobility-shift assay; ODN, (antisense) oligodeoxynucleotide; rer, rough endoplasmic reticulum; ser, smooth endoplasmatic reticulum; sw, salt-wash proteins from microsomes; swp, pellet obtained from sw; 3′UTR, 3′-untranslated region.

[1] To whom correspondence should be addressed.

In all subsequent steps, samples were kept on ice and centrifugation was at 4 °C. The homogenate was centrifuged at 10000 ***g*** for 10 min; the pellet was used to prepare nuclei and the supernatant was used to prepare microsomes, smooth (ser) and rough endoplasmic reticulum (rer), cytosol, free polysomes and ribosomes [21]. The pellet of the 10000 ***g*** centrifugation containing nuclei, mitochondria and debris was resuspended in nuclei buffer (homogenization buffer containing 2.5 mM $CaCl_2$ and 0.6 M instead of 0.25 M sucrose) and layered over a cushion of nuclei buffer containing 2.3 M sucrose. After centrifugation for 1 h at 100000 ***g***, the supernatant and debris (the layer above the pellet) were removed and the nuclei were resuspended in nuclei buffer, re-centrifuged at 100000 ***g*** for 30 min and resuspended in a small volume of the same buffer without Ca^{2+}. The postmitochondrial supernatant (after 10000 ***g*** centrifugation) was centrifuged at 100000 ***g*** for 1 h. The supernatant of this centrifugation was either mixed with 10 % (v/v) glycerol and retained (cytosol 1) or re-centrifuged at 150000 ***g*** for 1 h and the supernatant was adjusted to 10 % (v/v) glycerol for storage (cytosol 2). The pellet containing the free cytosolic ribosomes was resuspended in polysomal storage buffer [0.1 M potassium phosphate buffer, pH 7.4/1 mM DTE/20 % (v/v) glycerol containing the proteinase inhibitors (200 μg/ml of Pefabloc, 5 μg/ml of leupeptin and 1 μg/ml of aprotinin]. Cytosols 1 and 2 gave essentially the same pattern of cross-linked bands (results not shown). Microsomes were obtained from the pellet of the 100000 ***g*** centrifugation step as described by Camus et al. [8]. Briefly, the pellet was resuspended in a large volume of microsomal storage buffer [0.1 M potassium phosphate buffer, pH 7.4/1 mM K_2EDTA/1 mM DTE/20 % (v/v) glycerol containing proteinase inhibitors (250 μg/ml of Pefabloc, 5 μg/ml of leupeptin, 5 μg/ml of pepstatin and 1 μg/ml of aprotinin] and was re-centrifuged at 100000 ***g*** for 1 h. The resulting washed microsomal pellet was resuspended in microsomal storage buffer and stored for analysis. Polysomes, ser and rer were prepared by centrifugation of the washed microsomes through a discontinuous sucrose gradient [21]. The resulting ser and rer fractions were adjusted to 10 % (v/v) glycerol and polysomes, contained in the pellet, were resuspended in polysomal storage buffer. Aliquots of the fractions were stored at −70 °C immediately after preparation.

Preparation of microsomal salt wash proteins (sw)

Microsomal sw was prepared as described by Ross et al. [22] for the preparation of polysomal salt wash. The microsomal fraction was brought to 600 mM NaCl by slowly adding 2 M NaCl in 10 mM Hepes, pH 7.8, containing the protease inhibitors described above, the solution was gently mixed and left on ice for 15 min. Subsequently the solution was layered over a 30 % (w/v) sucrose cushion and centrifuged at 100000 ***g*** for 1 h at 4 °C. The supernatant was dialysed against RNA-binding buffer [10 mM Hepes, pH 7.5/1 mM $MgCl_2$/60 mM KCl/2 mM DTE/5 % (v/v) glycerol] until a concentration of 60 mM NaCl was reached (measured by ion conductance; Radiometer, Copenhagen, Denmark) and was stored at −70 °C. The pellet of the centrifugation was resuspended in RNA–protein binding buffer, brought to 60 mM NaCl in RNA binding buffer by dialysis and stored at −70 °C as microsomal salt-wash pellet (swp). Protein concentrations were determined using the Bio-Rad assay (Bio-Rad, Munich, Germany) with BSA as standard.

DNA templates and oligonucleotides

The plasmid used to generate CYP2A5 cDNA subclones was kindly provided by Dr. Negishi (Research Triangle Park, NC, U.S.A.) and contained an almost full-length cDNA clone of *CYP2A5* in pBluescript [23]. Full-length cDNA was subdivided into three parts (Figure 1) by digesting the plasmid with *Cla*I (MBI Fermentas, St. Leon-Rot, Germany). pBluescript SK II(+) (Stratagene, Heidelberg, Germany) was used as a cloning vector for subcloning. p3′UTR was created by subcloning the 278 bp *Cla*I fragment into the *Cla*I site of the cloning vector; pCDS (representing the major part of the coding sequence, see Figure 1) was made in a similar manner by cloning the 941 bp *Cla*I fragment into the same *Cla*I site. pEx1-3 was constructed by religating the remaining plasmid containing the 478 nt at the 5′ end of the cDNA after *Cla*I digestion of pBluescript SK II (7–17 nt missing at the 5′ end, Lindberg et al. [2], depending on the transcription start site). p3′UTR of c-*jun* was obtained as a subclone from plasmid AH 119 representing a mouse c-*jun* cDNA clone, a gift from Dr. G. Kinsley (DKFZ, Division of Molecular Biology of the Cell, Heidelberg, Germany) [24]. AH 119 was digested with *Eco*RI and *Sca*I and the ends of the resulting 1113 bp fragment were blunted with Klenow fragment and desoxynucleotides; this fragment was then introduced into the *Eco*RV site of pBluescript. Plasmid pSR5 (kindly provided by Dr. R. Leube, DKFZ, Division of Cell Biology, Heidelberg, Germany) was used as the cDNA clone for the generation of non-specific RNA transcripts; it contains the entire coding region of rat synaptophysin and small parts of its 5′ and 3′ non-coding regions (965 bp; [25]). The orientation and sequence integrity of plasmids pCoh, p3′UTR and pc-*jun* 3′UTR was confirmed by sequencing from both ends with dideoxynucleotides and sequenase 2.0 (United States Biochemical Corporation) following instructions of the supplier. The 70-nt sequence (nt 1610–1680 in [2]) was prepared by PCR as described by Geneste et al. [18]; oligodeoxynucleotides complementary to parts of the 70-nt sequence were kindly provided by Professor O. Pelkonen, Department of Pharmacology, University of Oulu, Finland.

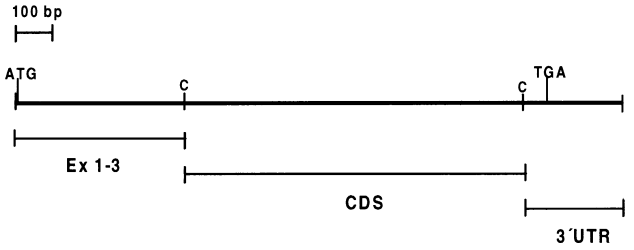

Figure 1 Map of the full-length mouse CYP2A5 cDNA clone

Full-length mouse CYP2A5 cDNA clone in pCoh and the positions and lengths of the three subclones (Ex 1-3, CDS and 3′UTR) produced from it. C, *Cla*I site used to generate the subclones; ATG, start of coding region; TGA, end of coding region.

Sequences of the antisense oligodeoxynucleotides (ODN) used

For location of the ODNs see positions indicated and [2]: *CYP2A5* ODN I: 5′ GAAATATCCTCTGCAAGTCTAC 3′ (nt 1631–1610); *CYP2A5* ODN II: 5′ TTCCCTCTTCTTTGGCTACCTTT 3′ (nt 1654–1632); *CYP2A5* ODN III: 5′ ATTCCTATTGACAACATAGTA 3′ (nt 1680–1660); scrambled sequence 5′-TGGCTTCTACATCCCCAAGAAAT-3′.

Preparation of RNA transcripts

Plasmids that served as templates for *in vitro* transcription were linearized by incubation with an appropriate restriction endonuclease that excises 3′ of the template sequence in the multiple

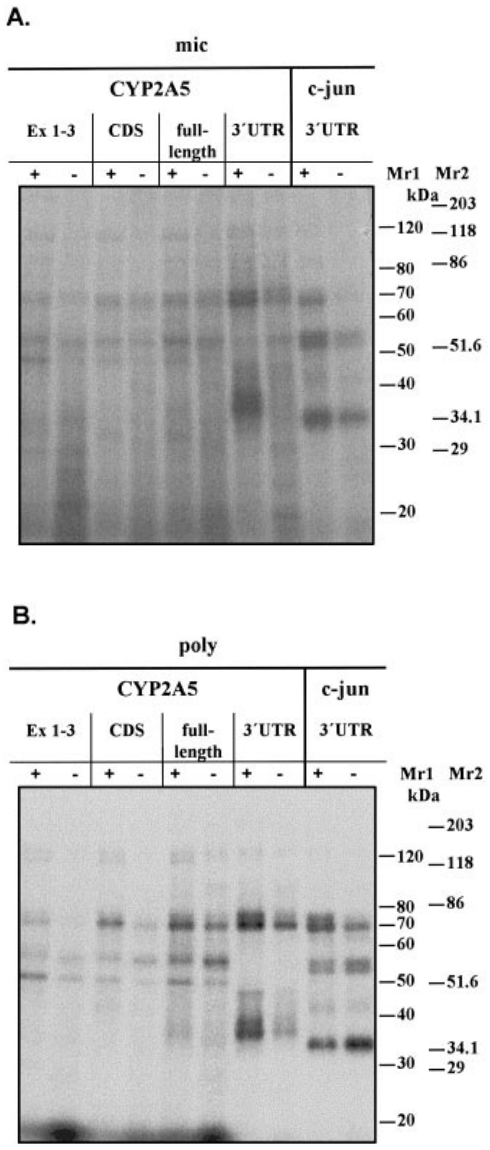

Figure 2 UV cross-linking assay with microsomal and polysomal proteins from pyrazole-treated mice

Binding of (**A**) microsomal proteins (mic) and (**B**) free polysomal proteins (poly) from untreated (−) and pyrazole-treated (+) mice to different parts of ^{32}P-labelled CYP2A5 mRNA and to the 3′UTR of c-*jun*; identical amounts of total protein (35 μg for microsomes, 33 μg for polysomes) were used for all probes. Labelled RNAs were used at identical molar concentrations. Molecular-mass (Mr) markers are shown on the right.

cloning site of the cloning vector. Aliquots of the product were monitored for complete cleavage on agarose gels. Large quantities of unlabelled RNA transcripts were produced and purified according to the manufacturer's instructions (Megascript kit; Ambion) using T3 or T7 RNA polymerase. Radioactively labelled RNA transcripts were synthesized by incorporation of [α-^{32}P]UTP (800 Ci/mmol; Amersham) into reaction mixtures following the method of Melton et al. [26]. Transcripts were separated from un-incorporated nucleotides by microdialysis on Millipore filters, type VS (0.2 μm). All transcripts were checked for quality on 2 % Mops–agarose gels or, for smaller transcripts (< 600 b), on 5 % (w/v) polyacrylamide gels containing 2.3 M urea using standard conditions [27]. Specific activities were determined by the radioactivity in 1 μl of dialysed RNA solution; usually ~ 3 ng of RNA were equivalent to 2×10^6 c.p.m.

RNA–protein binding reactions

RNA–protein binding reactions were performed as described previously [18], except that subcellular fractions were used preferentially. In brief, the reaction was routinely carried out in 20 μl (final volume) containing proteins (5–35 μg), 2×10^6 c.p.m. of ^{32}P-labelled RNA probe (~ 3 ng), 10 mM Hepes, pH 7.5, 1 mM $MgCl_2$, 60 mM KCl, 1 mM DTE, 5 % (v/v) glycerol and 5 μg of yeast tRNA, to prevent non-specific binding (unless otherwise noted). Different RNA probes were used at identical molar concentrations. The protein character of the factors binding to the RNA species used was evident from the necessity to include protease inhibitors for optimal binding results, and from an experiment in which cross-linking was prevented by heating the cellular subfractions (results not shown). In competition experiments with unlabelled sense RNA, the RNA, at the molar concentrations indicated, was added 5 min before the radiolabelled probe. In experiments with antisense probes, the ODN was pre-mixed with the ^{32}P-labelled RNA probe to allow base-pairing for 5 min before the addition of microsomal fractions from pyrazole-induced liver. RNA–protein binding was allowed to take place for 20 min at room temperature before direct loading onto native polyacrylamide gels for the GMSA or UV irradiation for the cross-linking assay.

Dependence of specific RNA–protein binding on monovalent cation concentration and on DTE

To ensure optimal binding conditions of ^{32}P-labelled RNA probes to proteins in cellular subfractions, formation of RNA–protein complexes was performed at different concentrations of monovalent cations. The 3′UTR-specific RNA binding for proteins from pyrazole-treated livers was sensitive to NaCl or KCl concentrations above 100 mM; 60 mM KCl or NaCl gave optimal results for high-signal intensity and maximal number of high-affinity bands in the binding pattern. In general, saturating amounts of proteins for RNA probes were used. To eliminate non-specific RNA binding, all binding reactions were performed in the presence of excess tRNA (*Escherichia coli*). When microsomes, prepared in buffer containing 1 mM DTE, were pre-incubated under RNA-binding conditions but without RNA for 20 min at 30 °C, a strong enhancement of signal intensity was observed when compared with samples left on ice. We concluded that DTE, present in the binding buffer, might activate pre-existing proteins under these conditions, as described for DNA binding proteins by Arnone et al. [28]. For further experiments, subcellular fractions were therefore prepared with buffers containing 2 mM DTE.

UV cross-linking assay

After the RNA–protein binding reaction (see above), reaction mixtures were placed on ice and exposed to UV light for 6 min at a distance of ~ 10 cm in a Stratalinker apparatus (Stratagene, Heidelberg, Germany). Subsequently, unbound RNA was digested for 30 min by 5 μg RNase A (5 μg/μl; Sigma) at 37 °C. Samples were analysed by SDS/PAGE (6–13 % acrylamide gradient) under standard reducing conditions. One or two sets of the following molecular-mass markers were always included in the gels: broad-range prestained marker proteins (Bio-Rad, Munich, Germany); the 10 kDa protein ladder (Gibco-BRL, Eggenstein, Germany); rainbow-coloured protein (14–220 kDa;

Amersham). After drying, the gel was exposed to X-ray film (Amersham). Radioactivity of detected proteins was quantified directly by PhosphoImager analysis (Imagequant, Krefeld, Germany) or indirectly by densitometry of autoradiographs (GS 670 Imaging Densitometer; Bio-Rad, Ivry-sur-Seine, France).

GMSA and analysis of shifted complexes

Binding reactions were carried out as described above. RNase T1 (20 units) (Ambion, Frankfurt, Germany) was added and the reaction mixture was incubated for 20 min at 37 °C. RNA–protein complexes were resolved in 5% non-denaturing polyacrylamide gels (acrylamide/methylene bisacrylamide, 37.5:1) with 50 mM Tris/glycine (pH 8.8) as running buffer. Radioactivity was detected by autoradiography of the dried gel. Further analysis of RNA–protein complexes was performed as described previously [29]. Samples, after the binding reaction, were UV cross-linked for 6 min (see above), incubated with RNase T1 and separated by PAGE (5% acrylamide). The band-shifted complexes were identified on a wet-gel autoradiogram and were excised from the gel on the basis of the autoradiographic pattern. Gel slices were then digested with RNase A (5 mg/ml) for 25 min at room temperature. Intact gel slices were transferred to fresh tubes containing 1 × Laemmli sample buffer and were boiled for 5 min before SDS/PAGE (6–13% acrylamide gradient). Where indicated, whole lanes were excised without previous autoradiography and were treated in the same way as the gel slices.

RESULTS

UV cross-linking shows enhanced protein binding to different parts of CYP2A5 mRNA and to the 3′UTR of c-*jun* after pyrazole treatment

In the initial approach, the binding of proteins obtained from subfractions of male DBA/2 liver, to U-α^{32}P-labelled RNA probes was determined by UV cross-linking [18]. When male DBA/2 mice were pretreated with pyrazole, a model compound known to upregulate CYP2A5 by stabilization of the mRNA, enhancement (subsequently called induction, without reference to specific mechanisms) of RNA–protein interactions was observed when compared with non-induced animals.

Using microsomes and free polysomes, the patterns of labelled bands formed were similar in both cases, but were clearer for free polysomes. Five major pyrazole-inducible RNA–protein bands were formed with probes representing the full-length, exon 1-3 (Ex1-3) and a major part of the coding sequence (CDS) of

Table 1 ^{32}P-Labelled protein bands detected by UV cross-linking assay

^{32}P-Nucleotide-labelled protein bands from mouse liver polysomes (results from three or more independent experiments). 120 db = 120 kDa double band. *, for other c-*jun* 3′UTR-binding proteins, see bands in Figure 2. Abbreviations used: –, not detected; s, specific binding as studied by competition; ns, non-specific; i, binding inducible by pyrazole.

[^{32}P]RNA probes CYP2A5	^{32}P-Labelled protein bands (kDa)					
	37/39	45/48	50	55	70/72	120 db
Full-length	s, i	–	i, ns	ns	s, i	i
Ex 1-3	–	–	i, ns	ns	ns, i	i
CDS	–	–	i, ns	ns	ns, i	i
3′UTR	s, i	s, i	–	–	s, i	i
c-*jun* 3′UTR*	–	–	–	ns	s, i	i

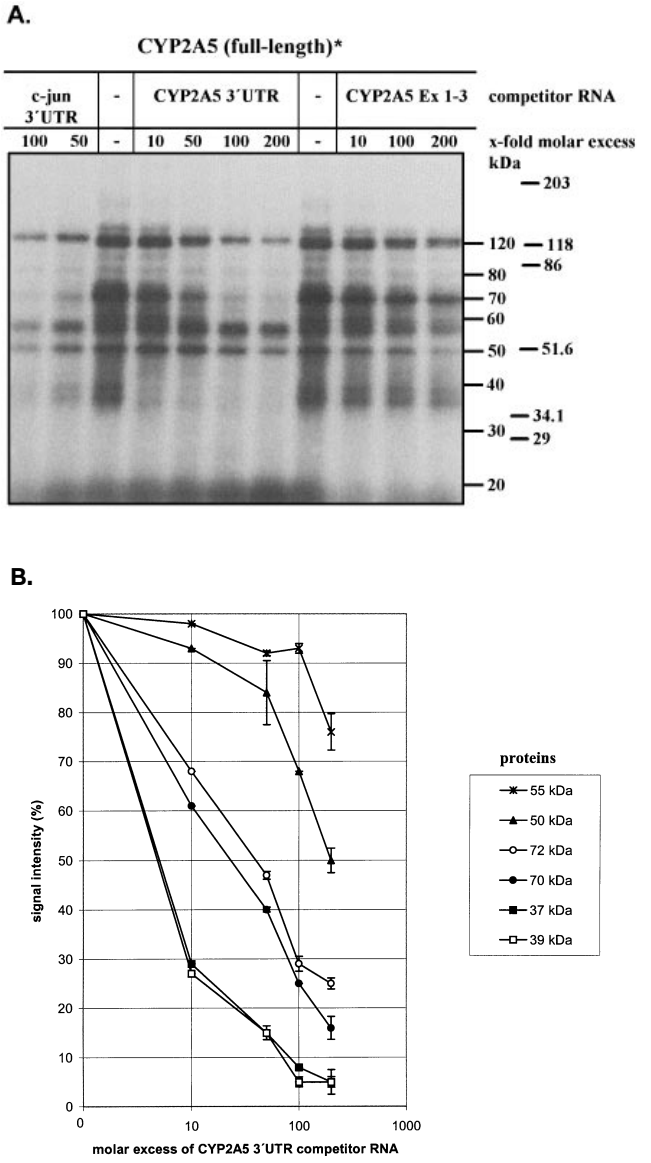

Figure 3 UV cross-linking assay showing the relative affinities of free polysomal proteins towards CYP2A5 full-length RNA

^{32}P-Labelled CYP2A5 full-length probe was used either alone (—) or in combination with increasing amounts of unlabelled competitor RNAs. (**A**) Autoradiography of the UV cross-linking gel. The asterisk indicates the radioactive probe. Molecular-mass markers are shown on the right. (**B**) Quantification of bands by phosphorimager. Mean values of two experiments are presented.

CYP2A5 mRNA: a double band at around 120 kDa, a 70/72 kDa doublet, bands around 55 kDa and a 50 kDa band. For the full-length probe weak labelling of bands at 37/39 kDa was also found (Figures 2A, 2B and Table 1). The 3′UTR probe cross-linked to the inducible bands at 70/72 and 120 kDa described above; in addition, it revealed an inducible strong doublet at 37/39 kDa (Figure 2) and an inducible doublet at 45/48 kDa. UV cross-linking of proteins to the Ex 1-3, CDS and full-length RNA probes was weaker when compared with results obtained with the 3′UTR.

Since strong enhancement of specific RNA–protein interaction was found after pyrazole treatment in the *CYP2A5* 3′UTR which contains two AUUUA elements [2], the 3′UTR of another

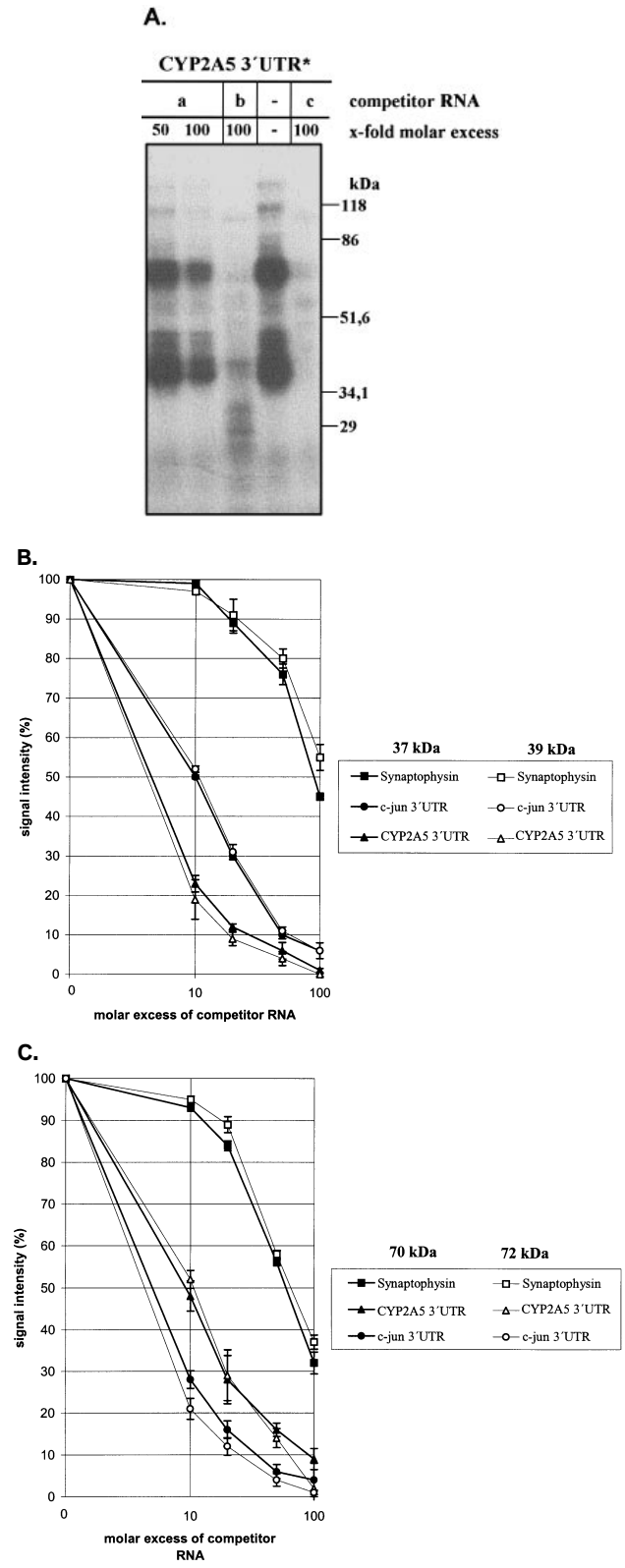

Figure 4 UV cross-linking assay showing the relative affinities of free polysomal proteins towards the 3′UTR of *CYP2A5*

^{32}P-Labelled *CYP2A5* 3′UTR probe was used either alone (—) or in combination with excesses of unlabelled competitor RNAs. (**A**) Autoradiography of the gel. The asterisk indicates the radioactive probe. (**B**) Quantification of the 37/39 kDa bands. (**C**) Quantification of the 70/72 kDa bands. Mean values of at least three different experiments are presented.

stress-inducible gene, c-*jun*, containing four AU-rich elements [24] was tested for binding of proteins. As shown in Figures 2A, 2B and Table 1, the c-*jun* 3′UTR also exhibited a specific pattern of RNA-binding proteins with high signal intensity, including the inducible 70/72 kDa doublet seen with the *CYP2A5* 3′UTR. However, the 35 and 53/55 kDa bands, typical of c-*jun* were not seen with *CYP2A5* 3′UTR; similarly, the strong 37–39 kDa bands, typical of *CYP2A5*, were not seen with c-*jun* 3′UTR. Although enhancement of the RNA–protein bands at 35 kDa and 70/72 kDa in microsomes from pyrazole-treated liver was also obtained with c-*jun*, this increase never exceeded a factor of two; in polysomes, the 35 and 53/55 kDa bands appeared weaker after pyrazole treatment. Taken together, these results suggest that some of the proteins interacting with the 3′UTRs are common to *CYP2A5* and c-*jun* while others are specific.

Relative affinities of the binding proteins

To test the affinity of protein binding and approach the question of specificity of different proteins for different RNAs in more detail, competition experiments were performed and band intensities were quantified by phosphorimaging. The relative affinities of the binding proteins were tested by competition with different parts of the CYP2A5 mRNA and the 3′UTR of c-*jun*, and by competition with an unrelated synaptophysin RNA probe (Figure 3 and Figure 4). Figure 3(A) shows the results obtained with a radiolabelled CYP2A5 (full-length) probe and different unlabelled RNA probes as competitors (exposure to the X-ray film was longer than that shown in Figure 2). As seen in Figure 3(B), the relative affinities of binding of CYP2A5 (full-length)-binding proteins to the competitor *CYP2A5* 3′UTR were 37/39 kDa > 70/72 kDa > 50 kDa > 55 kDa. The 55 kDa protein(s) was neither induced by pyrazole nor competed out very efficiently, indicating that it may be a general RNA-binding protein. Figure 4 demonstrates competition of the labelled *CYP2A5* 3′UTR by the non-radioactive synaptophysin mRNA, *CYP2A5* 3′UTR and c-*jun* 3′UTR. The 3′UTR c-*jun* probe proved to be a good competitor for the interaction of the 3′UTR *CYP2A5* with the 37/39 kDa bands, in contrast to the 70/72 kDa bands for which it was a better competitor than the *CYP2A5* 3′UTR itself (Figures 4B and 4C).

Subcellular distribution of binding proteins and relative levels of induction

The subcellular distribution of the proteins and their induction factors are summarized in Table 2. The relative order of band

Table 2 Induction of RNA–protein binding studied by UV cross-linking assay

Induction factors of protein bands in subcellular fractions (quantified with a phosphorimager). The induction factors are the means of at least three independent experiments performed with protein fractions from each of at least two different sets of treated animals (ribosomes were from one experiment only). Abbreviations used: ser, smooth endoplasmic reticulum; poly, free polysomes; rib, free ribosomes; mic, microsomes; rer, rough endoplasmic reticulum; cyt, cytosol.

	ser	poly	rib	mic	rer	cyt
37 kDa	2	2	2	5	2	4
39 kDa	2	2	2	5	2	3
48 kDa	1	2	2	3	1	2
70 kDa	1	2	2	2	1	2
72 kDa	1	2	2	2	1	2

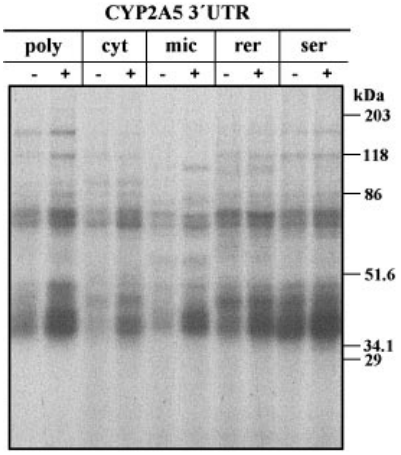

Figure 5 UV cross-linking assay showing the subcellular distribution and relative induction levels of *CYP2A5* full-length and *CYP2A5*-3′UTR RNA-binding proteins in pyrazole-treated (+) and untreated (−) animals

Subcellular fractions (35 μg of protein) of polysomes (poly), cytosol (cyt), microsomes (mic), rer and ser were used. A representative autoradiogram is shown. Molecular-mass markers are shown on the right.

intensities in fractions from pyrazole-induced liver was ser $\geqslant$ polysomes $\geqslant$ free cytosolic ribosomes $\geqslant$ microsomes $\geqslant$ rer $>$ cytosol (Figure 5; ribosomes not shown). With respect to pyrazole-inducible RNA binding, microsomes showed the highest induction for the 3′UTR-specific 37/39 kDa proteins and the 45/48 kDa proteins ($\geqslant$ 5-fold for the 37/39 kDa bands; see Figure 5 and Table 2). The induction factors for proteins binding to the Ex 1-3, CDS and full-length RNA probes in subcellular fractions did not exceed two (results not shown). Induction factors ranged between 2 and 3 only in free polysomes (e.g. induction factor 2.5 for the 50 kDa protein). Thus, with the exception of ser, the concentrations of specific binding proteins were particularly high in fractions containing polysomes or ribosomes. For this reason, microsomes were washed with 600 mM NaCl in buffer in order to release proteins associated with membrane-bound polysomes; the sw fraction indeed contained approx. three-fold increased levels (average 3.3, $n = 4$ experiments) of all specific binding proteins when compared with microsomes (see Figure 6).

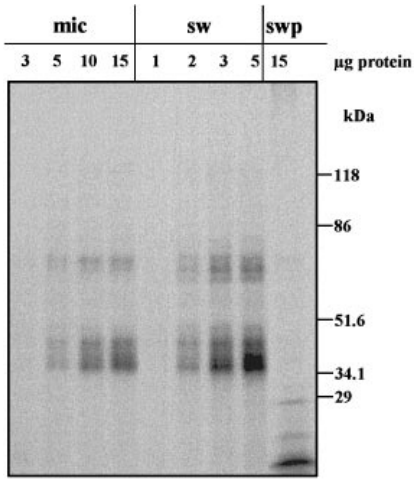

Figure 6 UV cross-linking assay of microsomal fractions

Binding patterns obtained with *CYP2A5*-3′UTR RNA and microsomes (mic), sw and the swp from pyrazole-treated animals. Different amounts of total protein were incubated with the same amount of ^{32}P-labelled *CYP2A5-3′*UTR RNA. Molecular-mass markers are shown on the right.

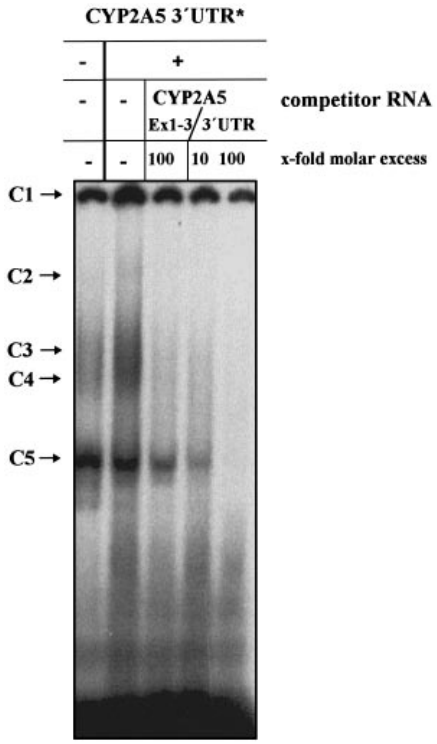

Figure 7 GMSA of free polysomal protein–RNA complexes

Complexes (C1–C5) formed from free polysomal proteins and ^{32}P-labelled *CYP2A5*-3′UTR RNA. +, Pyrazole-treated; −, untreated. Competition was performed with indicated molar excesses of Ex 1-3 and *CYP2A5*-3′UTR unlabelled RNA. The asterisk indicates the radioactive probe.

CYP2A5 mRNA-binding proteins detected by GMSA

RNA–protein binding was also studied by GMSA using the *CYP2A5* 3′UTR (Figure 7). At least five different complexes were identified with proteins from polysomes, four of them (C1–C4) were inducible by pyrazole treatment. On the top of the gel, a complex was observed that did not seem to enter into the gel matrix; this complex also showed increased signal intensity in samples from pyrazole-treated liver. Relative specificity of RNA–protein-interaction was indicated by competition with unlabelled RNA probes (Figure 7). Because other cellular subfractions also contained the *CYP2A5* 3′UTR-specific binding proteins as shown by UV cross-linking assays, GMSA was performed with polysomes, cytosol (150000 ***g***), free cytosolic ribosomes and the sw fraction. A complex, which showed the highest signal intensity was found in all fractions (indicated as C5 in polysomes, Figure 7). In addition, other complexes were seen which varied in intensity and position from fraction to fraction (Figure 8).

Analysis of shifted complexes

To identify proteins in different complexes and in complexes from different cellular subfractions, complexes were UV cross-

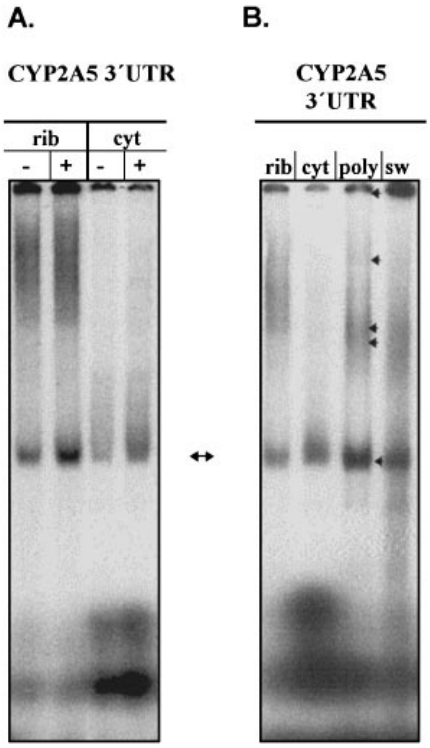

Figure 8 GMSA of subcellular protein–RNA complexes

Complexes of ^{32}P-labelled *CYP2A5*-3′UTR RNA with proteins of subcellular fractions: rib, free ribosomes; cyt, cytosol; poly: free polysomes and sw. (**A**) +, Pyrazole-treated; −, untreated. (**B**) Comparison of different subcellular fractions. The double arrowhead indicates the position of the smallest pyrazole-inducible complex present in all fractions tested. The arrowheads indicate the positions of the different complexes observed with polysomal proteins (see Figure 7).

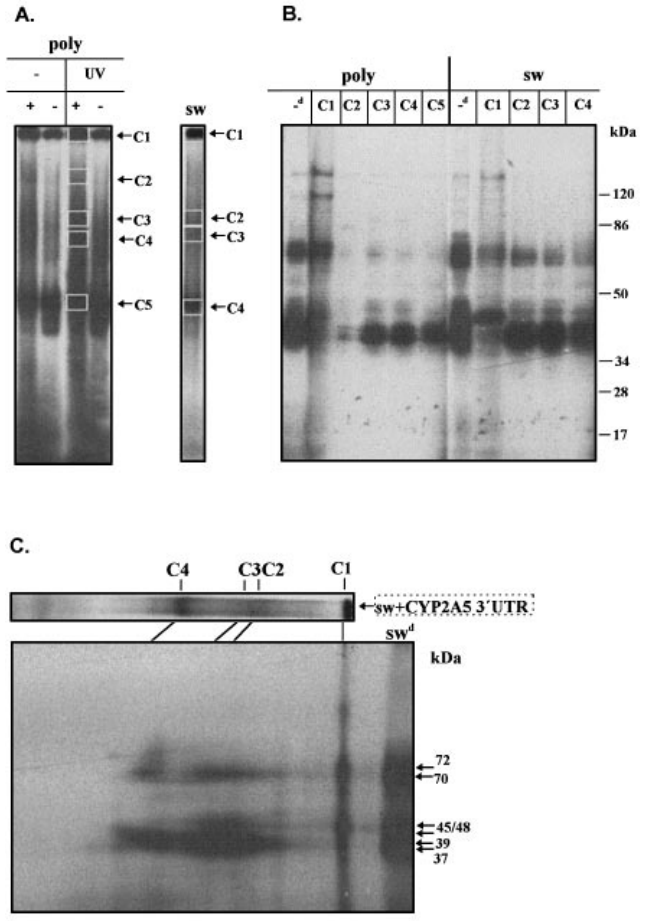

Figure 9 GMSA, RNase degradation and SDS/PAGE of polysomal protein–*CYP2A5*-3′UTR complexes

Identification of RNA-binding proteins present in *CYP2A5*-3′UTR complexes with polysomal proteins. (**A**) Autoradiograms of the GMSA. Comparison of complexes with polysomal protein (poly) from pyrazole-treated (+) and untreated (−) animals either UV-irradiated (UV) or non-irradiated (−). The positions of pyrazole-inducible complexes (C1–C5, see also Figure 7) are indicated by arrows and boxes. The positions of complexes formed with sw from pyrazole-treated liver (right panel) are also indicated by arrows and boxes (C1–C4). (**B**) Complexes poly C1–5 and sw C1–4 from (**A**) were excised individually from the wet gel, cleaved by RNase as described in the Materials and methods section and were resolved by SDS/PAGE into labelled bands. UV cross-linked bands, obtained in the usual way, are shown for comparison ($-^{d}$). Note the difference in signal intensities; lanes containing proteins from the direct UV cross-linking reactions ($-^{d}$) were exposed to the X-ray film overnight, whereas the rest of the gel was exposed for 3 days. (**C**) Analysis of complexes formed with sw proteins. The whole sw lane of the GMSA shown in (**A**) was excised, treated with RNase and placed on top of the SDS polyacrylamide gel before electrophoresis. sw^{d}, direct UV cross-linking reaction. Autoradiography after exposure for 2 days.

linked before loading on to the native gel. A similar complex pattern was obtained if proteins were either UV cross-linked to the RNA probe or not (Figure 9A; see also [29]). Gel pieces from the GMSA containing the RNA complexes formed with sw or free polysomes or the complete lane containing the RNA complexes with sw were excised and treated with RNase A before single proteins were resolved on SDS/PAGE (Figures 9B and 9C). As already observed by You et al. [29], analysis of cross-linked complexes under these conditions resulted in only weak protein bands compared with results obtained in direct UV cross-linking assays. However, when polysomes and sw were used, the 37/39 kDa bands, the 45/48 kDa bands and the bands at 70/72 kDa were revealed in all complexes (Figure 9B). In addition, after longer exposure, one or two bands of higher molecular mass (> 100 kDa) that varied depending on complex and protein fraction were sometimes seen. The complex retained on the top of the gel (C1) showed the whole pattern of proteins seen with direct UV cross-linking assay (Figures 9B and 9C). The patterns obtained with gel pieces each containing a single complex were confirmed by excising the whole lane and treating and analysing it by SDS/PAGE in the same way (Figure 9C).

p37/39 and p70/72 bind to a 70-nt sequence in the *CYP2A5* 3′UTR

The 3′UTR of *CYP2A5* contains a 70-nt sequence with one AUUUA motif and a probable hairpin loop as predicted by computer analysis [18]. When binding of proteins to this specific 70-nt sequence was tested by UV cross-linking, strong bands at 37/39 kDa in addition to weak bands at 70/72 kDa were found (Figure 10). When ODN I was pre-hybridized to the labelled probe, a decrease in labelling of the 37/39 kDa and 70/72 kDa bands was found with increasing concentration of ODN I. When ODN II was present, no bands were detectable at either 37/39 or 70/72 kDa. Instead, bands at about 47 kDa and 77 kDa became visible, in addition to a smear along the lane. Increased, rather than decreased band intensities were obvious when either ODN III or the scrambled sequence were used.

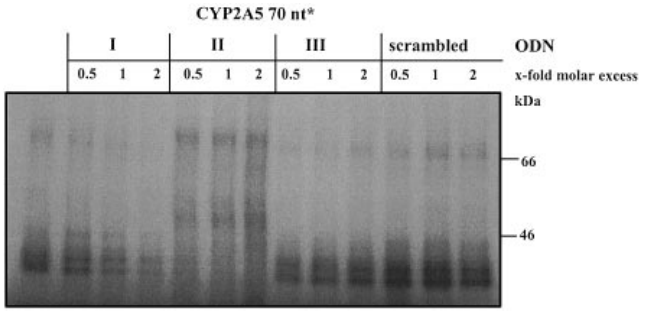

Figure 10 Effect of ODN on protein binding to the 70-nt loop

The indicated molar excesses of ODN I–III, and of a scrambled sequence were hybridized to ^{32}P-labelled 3′UTR of *CYP2A5* (10^6 c.p.m.), for 5 min before the addition of microsomal protein (5 μg) from pyrazole-treated mice.

Although specific binding proteins could be UV cross-linked to the 70-nt sequence, the 70-nt sequence did not form RNA–protein complexes in GMSA, indicating that a short-lived complex of RNA and proteins may exist, which can be fixed by UV cross-linking yet may not be stable enough for GMSA.

Exclusion of some candidate proteins

On the basis of our own and the results of others, initial attempts were made to identify or exclude candidates for the RNA-binding proteins. Gorospe and Baglioni [30] have reported the presence of five different AUUUA-binding proteins in rabbit reticulocyte lysate. These proteins ranged from 30–115 kDa and influenced the stability of interleukin-1α RNA in rabbit reticulocyte lysate. Recently, Ostareck et al. [31] have identified two 43 and 66 kDa proteins in rabbit reticulocyte precursors that bind to the mRNA of 15-lipoxygenase, regulating its stability and translation. Thus *CYP2A5* 3′UTR-binding proteins were sought in a rabbit reticulocyte system by UV cross-linking but no *CYP2A5* 3′UTR RNA-binding protein was detected under standard assay conditions. Uracil glycosylase, the monomer of glyceraldehyde-3-phosphate dehydrogenase, with a molecular mass of 37 kDa is also known to interact with some mRNAs [32], but could be excluded since, neither cross-linking of *CYP2A5* 3′UTR in the presence of the rabbit muscle enzyme (Boehringer, Mannheim, Germany) nor addition of the enzyme to mouse liver microsomes gave enhanced binding (results not shown).

DISCUSSION

The hepatic level of mouse CYP2A5 mRNA has been found to be increased post-transcriptionally by pyrazole, which is one of the strongest and most selective inducers of CYP2A5 [15–17]. After pyrazole treatment of mice, the CYP2A5 mRNA half-life increases from approx. 1.5 h to 6 h; the mechanism of this stabilization is unclear. Recently, a broad 44 kDa protein band was described, which was formed by UV cross-linking with the particular U-^{32}P-α-labelled 70-nt region of *CYP2A5* 3′UTR used in the present work. The protein giving this broad band was pyrazole-inducible and previous evidence suggests that it could play some role in the stabilization of the mRNA [18].

In the present report, we expanded the studies on proteins binding to CYP2A5 mRNA and show that, in fact, a number of different pyrazole-inducible proteins from male DBA/2N mouse liver bind with high affinity to different parts of the CYP2A5 mRNA. It remains to be seen whether these proteins are newly synthesized (‘induced’) or are modified forms of pre-existing proteins. A high binding affinity and some degree of specificity for some of the proteins was shown by competition with identical and non-related RNA sequences respectively. Thus the *CYP2A5* 3′UTR cross-linked preferentially to a 37/39 kDa doublet, to proteins at 45/48 kDa in addition to a 70/72 kDa doublet and a weak doublet at about 120 kDa. With the full-length mRNA, formation of all bands, especially that of 37/39 kDa, was weaker and two additional bands at 50 kDa and 55 kDa were found. This suggests that structural features of the full-length CYP2A5 mRNA–protein complex may modify the binding; there may also be a competition of different parts of RNA for binding factors. GMSA and GMSA–UV cross-linking assays confirmed the pyrazole-inducible proteins mentioned in this report. In addition they demonstrated that proteins in bands at 37/39, 45/48 and 70/72 kDa may be involved in a core complex structure to which other proteins may attach. Proteins that give rise to the labelled 37/39 kDa bands seem to bind with high affinity to the 20-nt loop of the 70-nt region (see Figure 10, and [18]) and its flanking regions, which contain an AU-rich site, and this provides a very interesting aspect in view of the suggested binding of RNA-stabilizing/destabilizing proteins to AU-rich sequences [29,33]. These binding characteristics were demonstrated using ODN I, II and III (see the Materials and methods section). ODN II, which binds to the presumed 20-nt loop containing a single uridine residue, inhibited labelling of the strong bands at 37/39 kDa more efficiently than ODN I whereas, different from ODN I, the 37/39 kDa and 70/72 kDa bands disappeared completely at a very low molar excess and new bands became apparent. ODN III and the scrambled sequence increased binding of several proteins. The relationship of several of the mRNA-binding proteins described here to the 44 kDa protein described by Geneste et al. [18] is not exactly clear. However, based on its binding characteristics and inducibility by pyrazole, it may be identical with the 37/39 kDa proteins described in this report.

Zhang et al. [34] reported the existence of a 150–200 kDa complex containing the AUUUA-binding protein, AUF1, which is composed of a 37 and a 40 kDa protein. Proteins of similar molecular masses were also described by Hamilton et al. [35] and Nakamaki et al. [33]. The relationship of these proteins to those described in the present report is unclear.

It is noteworthy that, in addition to binding to the 3′UTR of *CYP2A5*, the proteins giving rise to bands at 70/72 kDa appear to bind with high intensity to the 3′UTR of c-*jun*, a stress-inducible oncogene with a very labile mRNA. The mouse c-*jun* 3′UTR used here contained four AUUUA motifs which are thought to mediate the rapid turnover of the mRNA [24]. Surprisingly, the *CYP2A5* 3′UTR-specific 37/39 kDa bands were not detected when c-*jun* 3′UTR was used to radioactively label RNA in UV cross-linking assays, yet non-radioactive c-*jun* 3′UTR proved to be a good competitor for the 3′UTR of *CYP2A5* in labelling of the 37/39 kDa bands. This finding might indicate that, although relatively specific for CYP2A5 mRNA, the 37/39 kDa band-forming proteins may still show some affinity for c-*jun* 3′UTR or for proteins binding to c-*jun* 3′UTR. It is noteworthy that binding of some other proteins to the c-*jun* element was enhanced in mouse liver, indicating that the c-jun mRNA may also be affected by pyrazole-induced stress.

The 37/39 kDa band-forming proteins, as well as several of the other CYP2A5 RNA-binding proteins, were found mainly in microsomes, ser, free polysomes and free cytosolic ribosomes. Localization to these subfractions is in agreement with the findings of others (for a review see [36]), that many RNA-binding proteins involved in specific RNA metabolism

are associated with fractions containing polysomes or ribosomes and, as also shown here, can be released by high salt concentrations.

Preliminary data on degradation of labelled *CYP2A5* 3′UTR RNA in the presence of microsomes from control and pyrazole-induced liver, reveal that some of the induced proteins may enhance the stability of the 3′UTR (M. Thulke-Gross, unpublished work). However, the role of individual proteins has to be addressed in future studies.

In conclusion, we have described high-affinity binding of various pyrazole-inducible proteins to different parts of the CYP2A5 mRNA. Several of these proteins may interact with each other to build up complexes with which more proteins might interact by protein–protein interaction. We are presently aiming at isolating some of the proteins with a view to describing their function(s) in stress-enhanced expression of Coh (*Cyp2a5*, mouse) and of c-*jun*.

The introduction to some methods by and discussions with Dr. Olivier Geneste (IARC, Lyon, France) are gratefully acknowledged.

REFERENCES

1 Raunio, H., Syngelma, T., Pasanen, M., Juvonen, R., Honkakoski, P., Kairalvoma, M. A. and Sotaniemi, E. (1988) Biochem. Pharm. **37**, 3889–3895
2 Lindberg, R., Burkhart, B., Ichikawa, T. and Negishi, M. (1989) J. Biol. Chem. **264**, 6465–6471
3 Miles, J. S., McLaren, A. W., Forrester, L. M., Glancey, M. J., Lang, M. A. and Wolf, C. R. (1990) Biochem. J. **267**, 365–371
4 Yamano, S., Tatsuno, J. and Gonzalez, F. J. (1990) Biochemistry **29**, 1322–1329
5 Crespi, C. L., Penman, B. W., Leakey, J. A. E., Arlotto, M. P., Stark, A., Parkinson, A., Turner, T., Steimel, D. T., Rudo, K., Davies, R. L. and Langenbach, R. (1990) Carcinogenesis **11**, 1293–1300
6 Yun, C. H., Shimada, T. and Guengerich, F. P. (1991) Mol. Pharmacol. **40**, 679–685
7 Yamazaki, H., Inui, Y., Yun, C. H., Guengerich, F. P. and Shimada, T. (1992) Carcinogenesis **13**, 1789–1794
8 Camus, A. M., Geneste, O., Honkakoski, P., Bereziat, J.-C., Henderson, C. J., Wolf, C. R., Bartsch, H. and Lang, M. A. (1993) Mol. Carcinog. **7**, 268–274
9 Pelkonen, P., Kirby, G. M., Wild, Ch. P., Bartsch, H. and Lang, M. A. (1994) Chem. Biol. Interact. **93**, 41–50
10 Emde, B., Tegtmeier, M., Hahnemann, B. and Legrum, W. (1996) Toxicology **108**, 73–78
11 Kirby, G. M., Pelkonen, P., Vatanasapt, V., Camus, A.-M., Wild, C. P. and Lang, M. A. (1994) Mol. Carcinog. **11**, 81–89
12 Kirby, G. M., Chemin, I., Montesano, R., Chisari, F. V., Lang, M. A. and Wild, C. P. (1994) Mol. Carcinog. **11**, 74–80
13 Satarug, S., Lang, M. A., Yongvanit, P., Sithithaworn, P., Mairiang, E., Mairiang, P., Pelkonen, P., Bartsch, H. and Haswell-Elkins, M. R. (1996) Cancer Epidemiol. Biomarkers Prev. **5**, 795–800
14 Kirby, G. M., Batist, G., Alpert, L., Lamoureux, E., Cameron, R. G. and Alaoui-Jamali, M. A. (1996) Toxicol. Pathol. **24**, 458–467
15 Aida, K. and Negishi, M. (1991) Biochemistry **30**, 8041–8045
16 Hahnemann, B., Salonpää, P., Pasanen, M., Maenpaa, J., Honkakoski, P., Juvonen, R., Lang, M. A., Pelkonen, O. and Raunio, H. (1992) Biochem. J. **286**, 289–294
17 Salonpää, P., Pelkonen, O., Kojo, A., Pasanen, M., Negishi, M. and Raunio, H. (1994) Biochem. Biophys. Res. Commun. **205**, 631–637
18 Geneste, O., Raffalli, F. and Lang, M. A. (1996) Biochem. J. **313**, 1029–1037
19 Bohmann, D., Bos, T. J., Admon, A., Nishimura, T., Vogt, P. K. and Tjian, R. (1987) Science **238**, 1386–1392
20 Angel, P. and Karin, M. (1991) Biochim. Biophys. Acta **1072**, 129–157
21 Dallner, G. (1974) Methods Enzymol. **31**, 191–201
22 Ross, J., Kobs, G., Brewer, G. and Peltz, S. W. (1987) J. Biol. Chem. **262**, 9374–9381
23 Squires, E. J. and Negishi, M. (1988) J. Biol. Chem. **263**, 4166–4171
24 Ryseck, R.-P., Hirai, S. I., Yaniv, M. and Bravo, R. (1988) Nature (London) **334**, 535–537
25 Leube, R. E., Wiedenmann, B. and Franke, W. W. (1989) Cell **59**, 433–436
26 Melton, D. A., Krieg, P. A., Rebagliati, M. R., Maniatis, T., Zinn, K. and Green, M. R. (1984) Nucleic Acids Res. **12**, 7035–7056
27 Sambrook, J., Fritsch, E. F. and Maniatis, T. (1989) Molecular Cloning: A Laboratory Manual, 2nd edn., Cold Spring Harbor Laboratory, Cold Spring Harbor, NY
28 Arnone, M. I., Zannini, M. and Di Lauro, R. (1995) J. Biol. Chem. **270**, 12048–12055
29 You, Y., Chen, C. Y. and Shyu, A.-B. (1992) Mol. Cell. Biol. **12**, 2931–2940
30 Gorospe, M. and Baglioni, C. (1994) J. Biol. Chem. **269**, 11845–11851
31 Ostareck, D. H., Ostareck-Lederer, A., Wilm, M., Thiele, B. J., Mann, M. and Hentze, M. W. (1997) Cell **89**, 597–606
32 Nagy, E. and Rigby, W. F. (1995) J. Biol. Chem. **270**, 2755–2763
33 Nakamaki, T., Imamura, J., Brewer, G., Tsuruoka, N. and Koeffler, H. P. (1995) J. Cell. Physiol. **165**, 484–492
34 Zhang, W., Wagner, B. J., Ehrenman, K., Schaefer, A. W., DeMaria, C. T., Crater, D., DeHaven, K., Long, L. and Brewer, G. (1993) Mol. Cell. Biol. **13**, 7652–7665
35 Hamilton, B. J., Nagy, E., Malter, J. S., Arrick, B. A. and Rigby, W. F. C. (1993) J. Biol. Chem. **268**, 8881–8887
36 Ross, J. (1995) Microbiol. Rev. **59**, 423–450

Received 6 October 1997/17 December 1997; accepted 22 December 1997